Design of photoactivatable inhibitors for spatiotemporal control of GEF activity

By

Sidney Lyayuga Lisanza

Submitted to the Department of Chemistry
as supplement to the requirements for the degree of

Bachelor of Science in Chemistry with Honors

at the

University of North Carolina at Chapel Hill

_____

Faculty Advisor

Abstract

Protein design methods have been applied to engineer novel protein folds, enzymes, and materials with atomic-level accuracy. However, little work has been done to apply it to engineer novel proteins that can be used in vivo to dissect biological processes. Here we utilize protein design to study the cellular signaling involved in cell motility. Cell motility is driven by the reorganization of the cytoskeleton, a process regulated by the Rho protein family of small GTPases. These molecules are activated at precise subcellular locations by guanine exchange factors (GEFs) with fine temporal control. Understanding the biological role of these molecules requires their investigation at the subcellular level in living cells. To this end, we developed photoactivatable GEF inhibitors to allow for the spatio-temporal control of these GTPases. The GEFs targeted in this work were GEF-H1 and the members of Vav family GEFs, specifically Vav2. The two serve orthogonal roles in cell motility, where GEF-H1 has GEF activity towards RhoA at the retracting edge, Vav targets Rac1 at the leading edge. Our computational work generated a library of GEF-H1 inhibitors, and two experimentally validated inhibitors for the Vav family displaying high specificity in silico.

Introduction

Cell movement is critical in development, immune surveillance, and wound healing. It usually becomes disrupted in cancer.[1)] Cell motility is driven by the reorganization of the cytoskeleton, a process regulated by the Rho protein family of small GTPases. There are 22 known human members of the Rho family. These molecules are activated at precise subcellular locations by switching between an inactive GDP bound state and an active GTP bound state. This control is conferred primarily by two regulatory families of proteins. GTPase-activating proteins (GAPs) increase the intrinsic GTPase activity of Rho GTPases therefore inactivating them. Guanine nucleotide exchange factors (GEFs) catalyze the exchange of GDP for GTP. GEFs and GAPs are extensively regulated subsequently dictating the activation and inactivation dynamics of GTPases with fine spatiotemporal control.[2)]

The Dbl family of RhoGEF targets Rho GTPases specifically. Each member contains a Dbl homology (DH) domain and an adjacent, C-terminal, pleckstrin homology (PH) domain. The DH domain is responsible for the activation of GTPases, while the PH domain is thought to localize DbI proteins to plasma membranes and to regulate GEF activity via allosteric interactions.[2)]

The GEFs of interest in this study are GEF-H1 and the Vav family of proteins. GEF-H1 is an activator of the Rho GTPase RhoA. RhoA plays a critical role at the advancing and retracting edges of moving cells.[3)] Active RhoA stimulates many downstream effectors, such as mDia1 that leads to actin polymerization and myosin II that leads to cell contraction.[4)] GEF-H1 knockdown results in decreased RhoA activation at the leading edge, impaired membrane protrusion, and significantly reduced motility in many different cell lines.[5)] GEF-H1 is the only known GEF that localizes at the microtubules in its inactive state and microtubule release leads to its activation.[1)]

Therefore, GEF-H1 couples microtubule dynamics with Rho GTPase activation and changes in the actin cytoskeleton.[5)]

The Vav family of proteins contains 3 isoforms: Vav1, Vav2, and Vav3. Vav1 is primarily expressed in hematopoietic cells, whereas Vav2 and Vav3 are more ubiquitously expressed. Vav proteins are thought to primarily target the GTPase Rac1. Rac1 is the primary regulator of actin cytoskeleton reorganization, where it mediates lamellipodia formation and membrane ruffles in response to extracellular signaling.[6)] Through knockdown studies it is known that Vav proteins are critical to T and B cell receptor responses propagating cytoskeletal rearrangement for processes including the formation of the immunological synapse, phagocytosis, and integrin mediated T-cell spreading.[7)]

Results

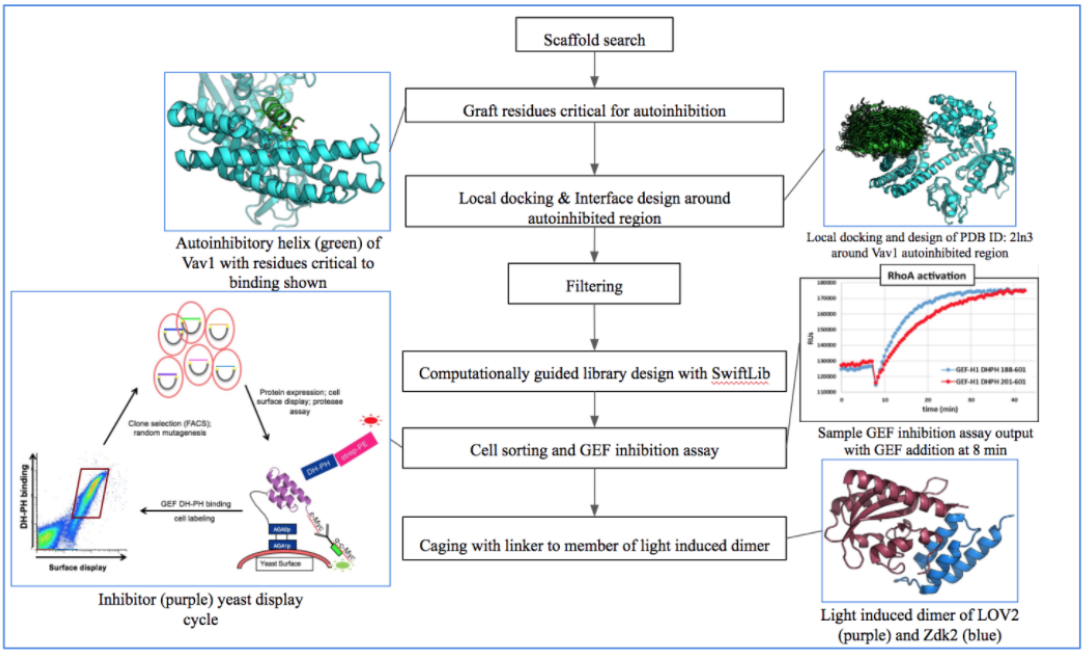

Figure 1: GEF inhibitor design pipeline

Computational generation of Vav inhibitor library:

To computationally model Vav2 we utilized the Vav1 crystal structure because of the high sequence homology between the two and the lack of a Vav2 crystal structure. Vav is autoinhibited by a helix, termed the AID , from its AC domain that binds to its catalytic DH domain. The computational approach used for inhibitor design used the Rosetta macromolecular modeling software[8)] to engineer scaffold proteins maintaining and adding to the contacts of the AID on the DH domain of Vav. Proteins containing helices that align well with the inhibitory helix were utilized. Zdark a 3 helical protein part of the LOV2/Zdark[9)] light inducible and reversible dimer was used as the scaffold to be engineered for Vav binding. Our modeling shows that LOV/Zdark complex formation will satirically block the interaction between Zdark and Vav, because of clashes between LOV and Vav. Light irradiation would cause the complex to dissociate, allowing the engineered inhibitors to bind to Vav and block its GTPase interaction, therefore conferring photo inhibition towards Vav. This LOV2/Zdark system has proven competent in controlling the localization and activity of proteins caged to them.[9)]

The residue critical for interaction is the central Tyr174 within the AC domain that makes contact with Arg332 within the DH domain to form a salt bridge. Tyr174 in addition toMet176 were grafted onto Zdark within a LOV2 non-interacting helix at position 49. Residues not interacting with LOV2 making contact with the active site were allowed to mutate during the computational modeling. Local docking and fine backbone movements[10)] of the Zdark around the active site was then undergone. To evaluate the ability of designs to fold and bind, we computationally filtered by Rosetta metrics such as the solvent exposed surface area (SASA), the binding energy (ddG), and the shape complementary (Sc) of the interface. The top 2,000 designs

passing filtering were used to construct a ~two million amino acid diverse library with the SwiftLib[8] software along with manual optimization.

Computational generation of GEF-H1 inhibitor library:

There is no crystal structure for GEF-H1, however the DH domain in DbI GEFs is highly conserved. We therefore computationally predicted the structure of the GEF-H1 DH domain by grafting the DH domain residues of GEF-H1 onto the backbone of the Vav1 crystal structure. Several rounds of side chain minimization and backbone perturbation were done to determine the GEF-H1 structure used for modeling. GEF-H1 sequence alignment with that of Vav shows AID homology in addition truncation experiments of the region show increased GEF activity towards RhoA (data not shown). Therefore the targeting of the DH domain strategy was employed once again.

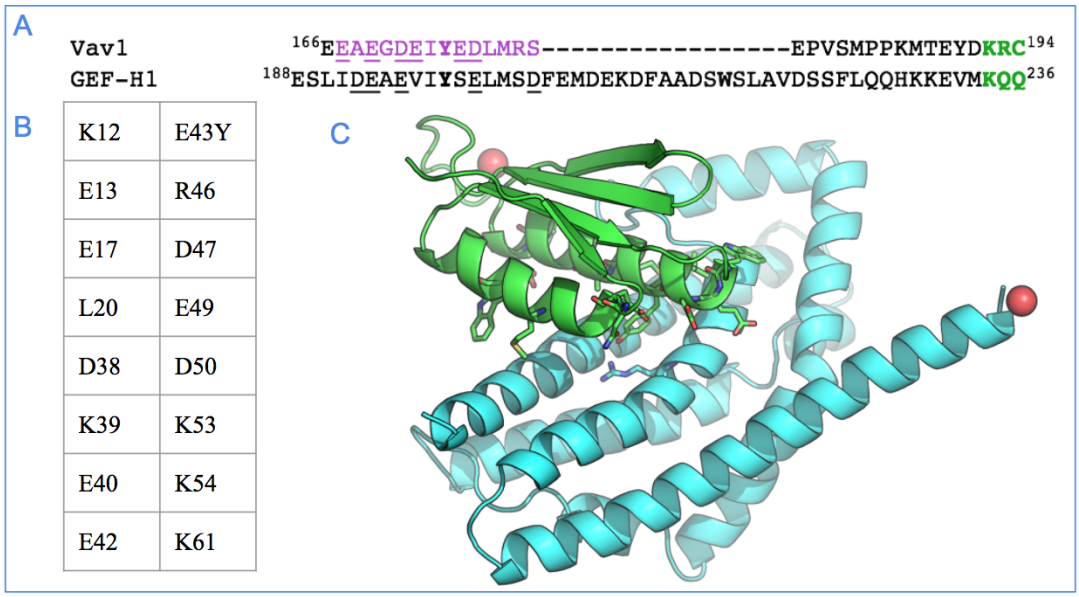

K12	E43Y
E13	R46
E17	D47
L20	E49
D38	D50
K39	K53
E40	K54
E42	K61

Figure 2: (A) Sequence alignment of Vav1 and GEF-H1 (B) Residues allowed to mutate on PDB ID: 2LN3 (C) 2lN3 (green) with residues allowed to mutate shown. Predicted GEF-H1 backbone (blue) with arg564 shown. Red ball indicates C terminal

The Protein Data Bank was mined for novel computationally engineered structures containing helices that align well with the inhibitory helix. Computationally designed proteins are

typically very stable, thus can support a large number of modification without affecting their stability, and should have minimal off target interactions *in vivo*. Initial work was with Zdark, but the generated inhibitors were nonspecific (data not shown). PDB ID: 2LN3 was chosen as the scaffold. 2LN3 is a de novo designed protein with ideal secondary structures displaying high thermal stability. Residues making contact with the active sight were allowed to mutate with position 43 set to tyr. Constraints were then set for Tyr43 on 2ln3 and Arg564 on GEF-H1 to maintain hydrogen bonding. The following computational protocol was utilized: docking of the two structures, sampling of different rotamers and amino acids for the allowed positions, followed by minimal backbone perturbation. Twenty thousand models were built, and the top 2,000 by ddG were used to generate a sequence profile from which a library was designed with SwiftLib along with manual inspection.

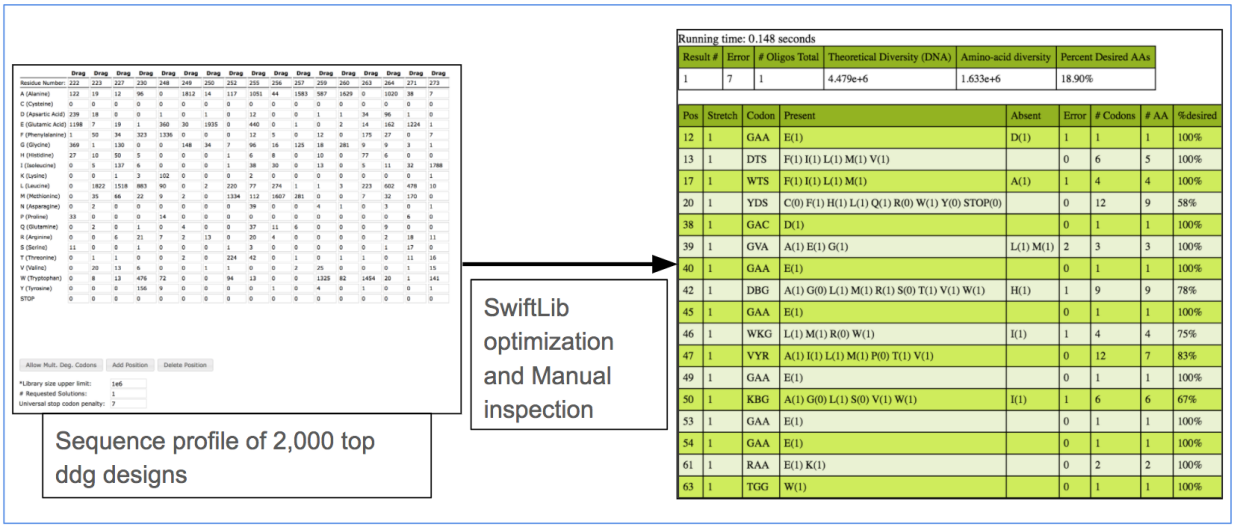

Running time: 0.148 seconds

Result #	Error	# Oligos Total	Theoretical Diversity (DNA)	Amino-acid diversity	Percent Desired AAs
1	7	1	4.479e+6	1.633e+6	18.90%

Pos	Stretch	Codon	Present	Absent	Error	# Codons	# AA	%desired
12	1	GAA	E(1)	D(1)	1	1	1	100%
13	1	DTS	F(1) I(1) L(1) M(1) V(1)		0	6	5	100%
17	1	WTS	F(1) I(1) L(1) M(1)	A(1)	1	4	4	100%
20	1	YDS	C(0) F(1) H(1) L(1) Q(1) R(0) W(1) Y(0) STOP(0)		0	12	9	58%
38	1	GAC	D(1)		0	1	1	100%
39	1	GVA	A(1) E(1) G(1)	L(1) M(1)	2	3	3	100%
40	1	GAA	E(1)		0	1	1	100%
42	1	DBG	A(1) G(0) L(1) M(1) R(1) S(0) T(1) V(1) W(1)	H(1)	1	9	9	78%
45	1	GAA	E(1)		0	1	1	100%
46	1	WKG	L(1) M(1) R(0) W(1)	I(1)	1	4	4	75%
47	1	VYR	A(1) I(1) L(1) M(1) P(0) T(1) V(1)		0	12	7	83%
49	1	GAA	E(1)		0	1	1	100%
50	1	KBG	A(1) G(0) L(1) S(0) V(1) W(1)	I(1)	1	6	6	67%
53	1	GAA	E(1)		0	1	1	100%
54	1	GAA	E(1)		0	1	1	100%
61	1	RAA	E(1) K(1)		0	2	2	100%
63	1	TGG	W(1)		0	1	1	100%

Figure 3: Library generation with SwiftLib and manual optimization

VAV Library Selection:

The Vav library generated was screened via yeast display.[11)] Constructs were expressed onto the surface of yeast as a fusion with the Aga2p protein. Display was measured by fluorescence labeling of a c-Myc epitope tag, while binding was measured with a biotinylated Vav2 DH/PH

domain labeled with a streptavidin conjugated fluorophore. Cells were selected by fluorescence activated cell sorting (FACS). Four rounds of selection were undergone with the first three running the Vav2 DH/PH domain at 2uM. The last round of selection required three independent sortings. The first being ran against the Vav2 DH/PH domain at 300 nM, the second with the GEF-H1 DH/PH domain at 300 nM, and lastly with 300 nm of the Vav2 DH/PH domain and 3uM of unlabeled GEF-H1 DH/PH domain. Selection was for constructs which showed binding towards Vav2, but not GEF-H1. Therefore, endowing some specificity towards Vav in addition to selecting against unfolded and nonselective binders.

The above resulted in the first inhibitor termed, VI1. From there a second library was generated with the initial sequence being from VI1 allowing further mutations at positions 48, 52, 53, 55, and 56. Two binders resulted from the library, VI120 and VI130.

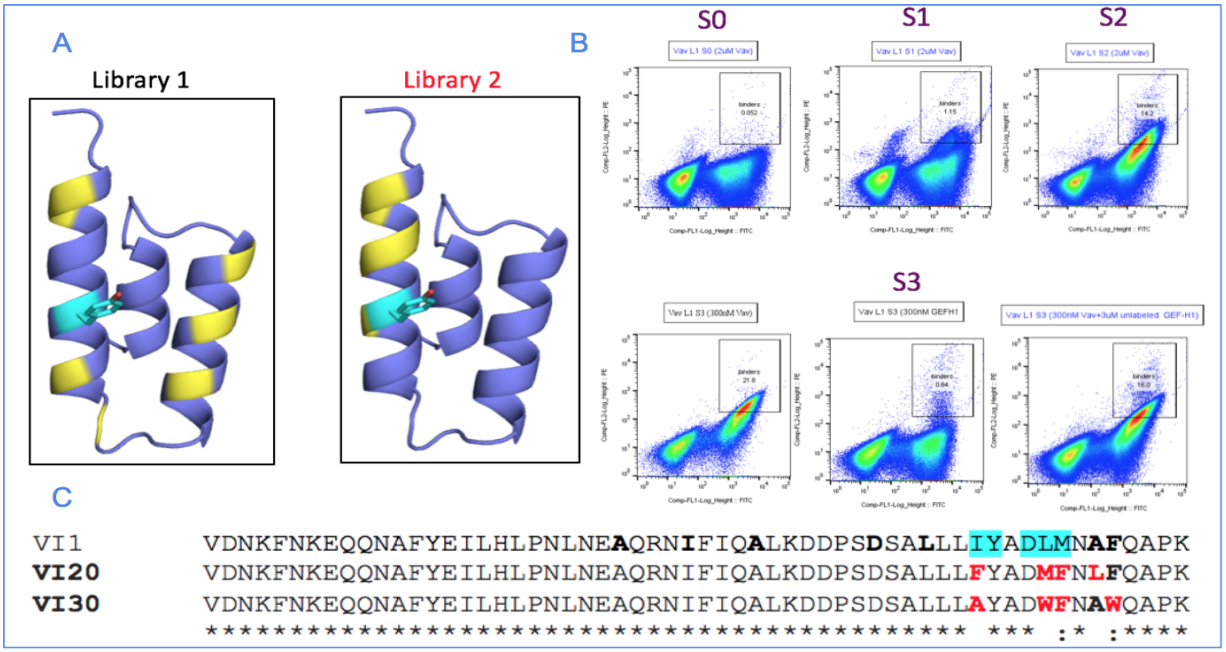

Figure 4: (A) Highlighted in yellow are sights allowed to mutate on Zdark in the initial and second library, with tyr49 shown (B) FACS data for selection of inhibitors from library 1 (C) Inhibitors found from library 1 and 2

VAV inhibitor and VAV DHPH physical characterization:

A 4xHis tag was introduced into the Vav2 DH/PH domain. Vav2 was expressed in *E coli* cells induced with IPTG for 36 hours at 18 C Purification was with a Ni2+ column. SDS-PAGE gel electrophoresis shows the presence of Vav2 at the expected molecular weight of ~45 kDa. The two above bands could be nonspecific binding of proteins from the cell lysate to the Ni^{2+} resin.

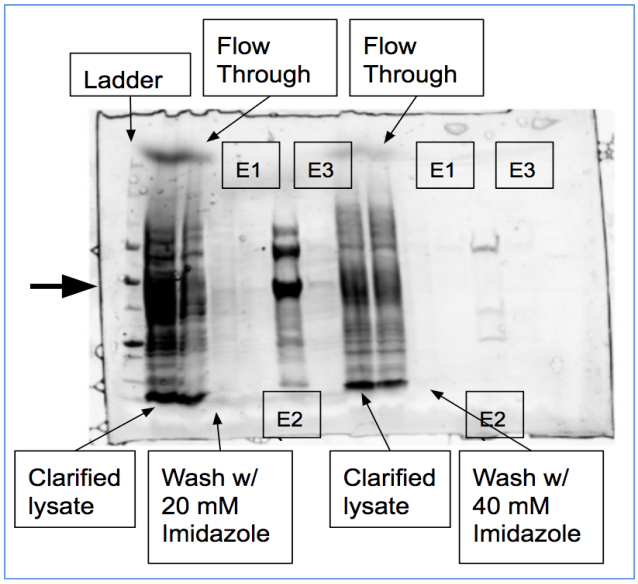

Figure 5: Vav2 DH/PH domain gel with bolded arrow indicating mass of interest

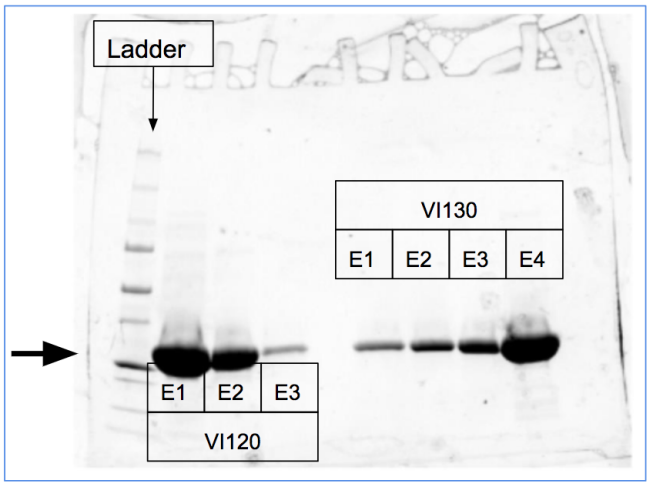

Figure 6: VI120 and VI130 gel with bolded arrow indicating mass of interest

VI120 and VI130 were tagged with Glutathione S-transferase (GST) and purified with a glutathione-imobilized (GSH) column. The inhibitors expressed well, the SDS_PAGE gel shows the inhibitors present at ~20 kda. and had high purity.

VAV inhibitor evaluation of GEF inhibition:

A GEF activity assay was used to test GEF inhibition by inhibitors as well as GEF activity for the purified Vav2 DH/PH domain. Within the assay, GDP fused to the fluorescent dye BODIPY is bound to a known VAV GTPase target, Rac1. Upon release of GDP-BODIPY fluorescence output is increased which was measured with a fluorometer therefore indicating the release of

GDP, and by extension GEF activity. To test the activity of the purified Vav2 DH/PH domain, different concentrations, 10uM and 5 uM, of the GEF was added to their respective GDP bound rac1 solutions each at the 27 min mark (Figure 7). Fluorescence increased promptly showing that the purified Vav2 maintained GEF activity. More so the higher concentration, 10 uM Vav2 showed a more robust response as compared to the 5 uM Vav2.

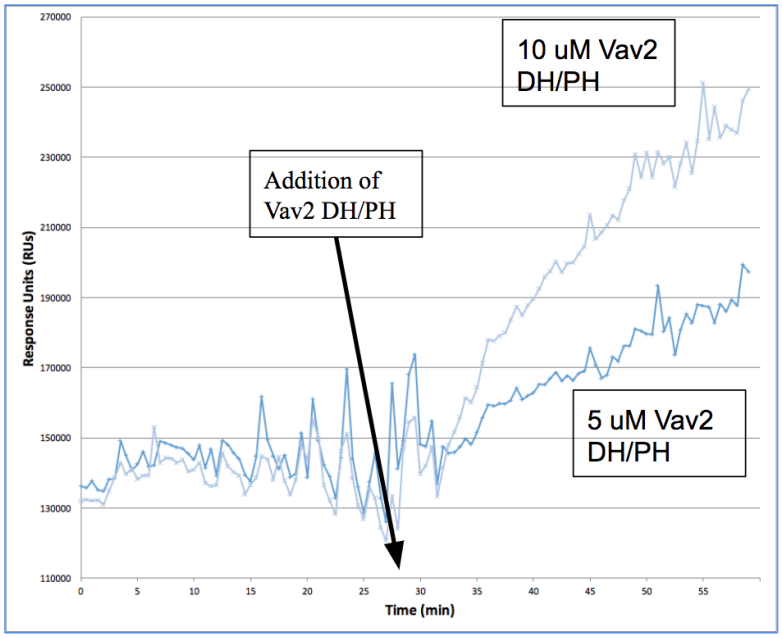

Figure 7: GEF inhibition assay with Vav2 addition at 27 min

To test the ability of the inhibitors to block Vav2-Rac1 interaction in vitro three separate GDP-BODIPY bound Rac1 solutions were prepared. Each received either Vav2, Vav2 and VI120, or Vav2 and VI130 (Figure 8). Note the difference in increase of fluorescence. Vav2 serving as the control has higher GEF activity as compared to the inhibitors. While VI120 and VI130 show a significant decrease in GEF activity at an equivalent level to each other.

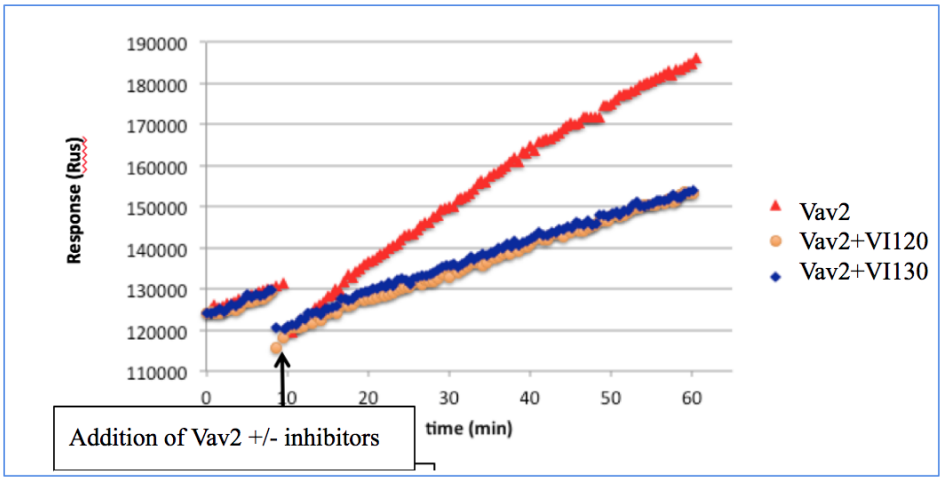

Figure 8: GEF inhibition assay with Vav2 +/- addition at 10 min

VAV inhibitor evaluation of binding affinity:

Binding affinity of the purified proteins was tested by surface plasmon resonance (SPR). Rac1, a known low nanomolar[12] affinity binder for Vav, was tested as a positive control. However binding could not be determined at 1 uM, 0.1 uM, and 0.01 uM due to the noise present in the data. Binding was detected at 100 uM, indicating that some portion of the purified Vav2 DH/PH domain on the gold film was unfolded under the experimental conditions.

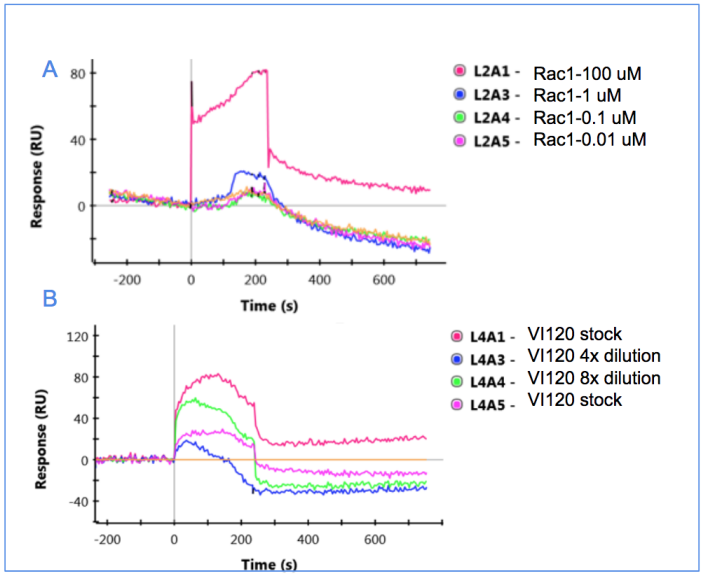

Figure 9: SPR data with the Vav2 DH/PH serving as the ligand and Rac1 (A) or VI120 (B) serving as the analyte

Utilizing the same Vav2 sample from the above experiment, VI120 was analyzed, with a stock concentration of 560 uM. A response was detected for the stock concentration in addition to both a 4x and 8x dilution. This indicates binding, but because of the noise within the system it is difficult to determine a dissociation. However, at our current detection levels (>10uM), VI120 appears to bind to Vav2 similar to Rac1.

Analysis

Modeling of VI120 and VI130 interaction

Both VI120 and VI130 were computationally modeled utilizing Rosetta to determine if binding affinity and specificity could be increased via the addition of further mutations. Here I will describe the work done with VI120. The following computational protocol was applied: The VI120 sequence was threaded onto the Zdark backbone, thereafter docking around the DH domain with hydrogen bond constraints on Zdark tyr49 and Vav arg332 was undergone. This was followed by packing of side chains and aggressive backbone movement for several rounds. Manual inspection of top ddG structures, with special attention to packing of the large hydrophobics introduced in the second library, determined the best model for the binding of VI120 on Vav. Modeling showed that at position 27 the alanine present did not pack well against the DH domain. That position was allowed to mutate within subsequent Rosetta computational runs, it was determined that the introduction of an isoleucine would best fit the cavity.

In Silico Binding specificity

To gauge the specificity of the designed Vav inhibitors, Vav homologues with known structures were found with the HMMER web server. 11 such GEFs were found. To test their potential to interact with Vav *in silico,* VI120 was docked against each structure's DH domain. 1000 models were generated for each, which were then scored for ddG. From this data (Figure 10), it is clear that VI120 has preference towards Vav. As a baseline, because the inhibitor were selected against GEF-H1, docking runs were also undergone with the computationally predicted GEF-H1 structure, and again preference is for Vav. A similar run was undergone with Rac1 in lieu of the inhibitors. There was a strong preference for Rac1 over the inhibitors as expected. To further our

specificity analysis we looked at the relative abundance of GEFs within the breast cancer cell line, MDA-MB-231, where these inhibitors will be used biologically. The most prevalent GEFs of close homology were PDZRhoGEF, LARG, p115, and GEF-H1. Likewise VI130 in addition to VI120 was docked against these most likely binders, and showed preference for Vav. Nevertheless our computational analysis indicates that both VI120 and VI130 may have significant binding toward PDZRhoGEF, LARG and p115. Therefore additional modelling and screening may be necessary to ensure absolute specificity, if such interactions are confirmed experimentally.

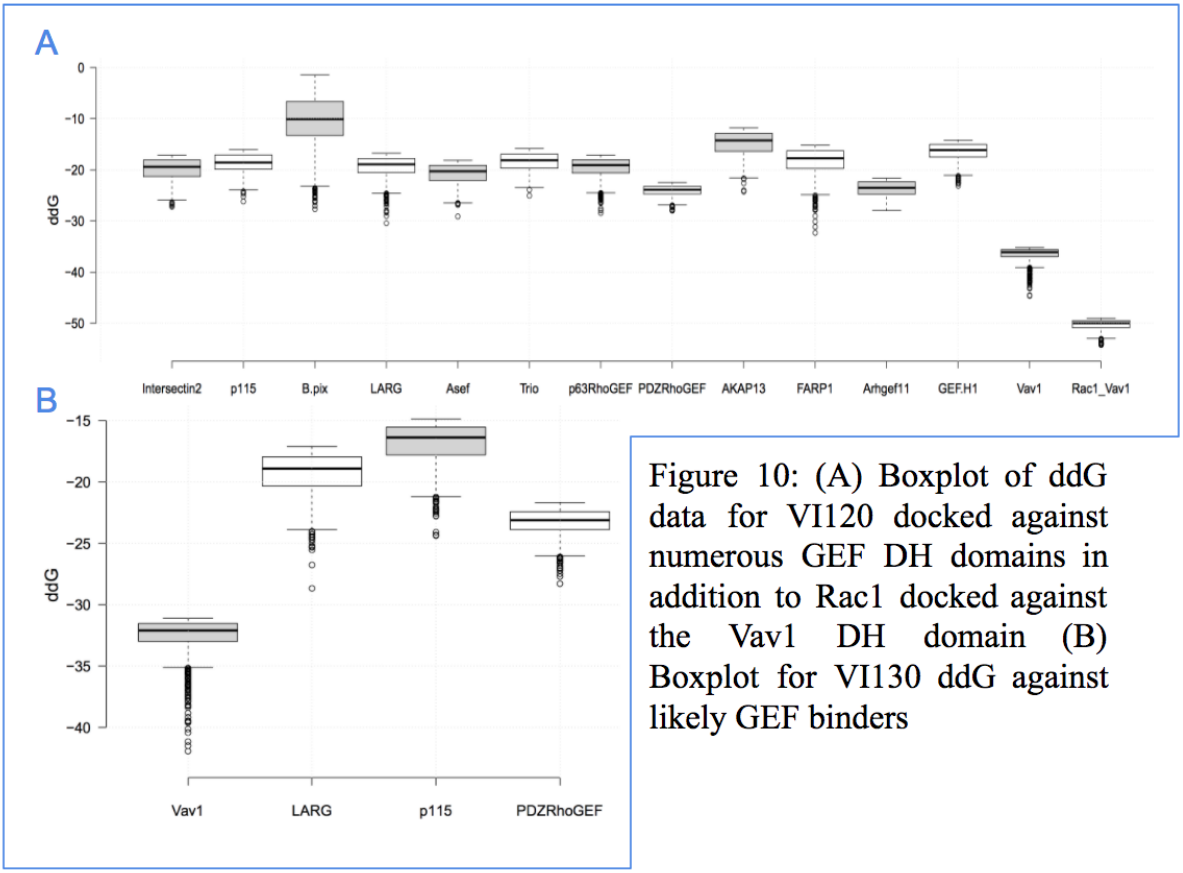

Figure 10: (A) Boxplot of ddG data for VI120 docked against numerous GEF DH domains in addition to Rac1 docked against the Vav1 DH domain (B) Boxplot for VI130 ddG against likely GEF binders

Future Directions:

GEF-H1

The designed library will need to be screened experimentally, employing the same procedure as Vav. Once binders have been found and characterized different light-dependent dimers such as LOV2/Zdark11 and CRY2/CIB1[13], will be fused to the engineered inhibitors such that dimer formation will occlude the GEF-H1 binding site. Upon light irradiation, the dimer will dissociate, allowing the inhibitors to bind to GEF-H1 and block GTPases interaction. Dimers will be fused at different site and with linkers of variable length to find constructs with optimal caging dynamics and inhibitory properties.

Vav2

Pull down assays for VI120 and VI130 will be undergone to determine if there are any unintended binders, with special focus on identifying the presence of PDZRhoGEF, LARG, and p115. In addition the GEF activity assay will be performed once again with the addition of both LOV light and dark state mutants. Where we expect the light state mutants to not interfere with GEF activity inhibition, while the dark state mutant should occlude inhibition because of dimer formation. From there the inhibitors will be expressed in the breast cancer cell line cell line, MDA-MB-231, to study the subcellular dynamics of Vav2.

Conclusion

The approach described in this thesis will allow the study of endogenous GEF-H1 and Vav2 with precise spatial and temporal control of activity. Other inhibition methods such as gene knockdown or RNAi do not provide such level of control and may lead to developmental and signaling artifacts in cells, which may confound biological findings. Furthermore, the inhibition can be applied reversibly. The approach described here is general and can be applied to develop inhibitors for the other 67 members of the Dbl family of GEFs. All these GEFs use a DH domain to activate GTPases, and in theory specific and potent inhibitors could be engineered against them

in the future. With the exception of one small molecule developed against LARG GEF, no inhibitors exist for GEFs. Given that GEFs have been found to be overexpressed in cancers[2)] , these molecules could be used to study the role of GEFs in driving metastasis or as potential therapeutics.

Methods

Proteins were designed with the Rosetta macromolecular modeling software. Library selection for binders was done with yeast display with binding dynamics characterized by surface plasmon resonance. Proteins were expressed in E. Coli and underwent purification either by a Ni column or a glutathione column.

Sample Rosetta Scripts

```
script used to generate models for 2ln3 binding to gefh1 with constraints
on h-bond with tyr43A and arg564B nstruct 10 with 2000 runs
<ROSETTASCRIPTS>
<SCOREFXNS>
</SCOREFXNS>
<TASKOPERATIONS>
       <InitializeFromCommandline name="ifcm"/>
       <ReadResfile name = "rrf" filename="clean_2ln3_gefh1.resfile"/>
       <RestrictToRepacking name="r2p"/>
</TASKOPERATIONS>
<FILTERS>
       <Sasa name="sasa" confidence="0"/> change confidence to 1 if you
want low-sasa structures ot be supressed
       <Ddg name="ddg" confidence="0"/>
</FILTERS>
<RESIDUE_SELECTORS>
    <Index name="tyr43" resnums="43A" />
    <Index name="arg564" resnums="564B" />
</RESIDUE_SELECTORS>
<MOVERS>
       <AddConstraints name="add_csts" >
                <HydrogenBondConstraintGenerator name="gen_my_csts"
                residue_selector1="tyr43"
                residue_selector2="arg564"
                atoms1="OH"
                atoms2="NH1"
                atom_pair_func="FLAT_HARMONIC 2.6 0.1 0.5" />
        </AddConstraints>
        <RemoveConstraints name="rm_csts"
constraint_generators="gen_my_csts" />
       <Backrub name="bckrub"/>
```

```
	<PackRotamersMover name="packer" task_operations="ifcm,rrf"/>
	<Docking name="dock1" fullatom="1" local_refine="1"/> make
fullatom=0 to do low-resolution only docking. Change local_refine=1 to do
only high-resoltuion docking
	<ParsedProtocol name="pack_dock" >
		<Add mover_name="dock1"/>
		<Add mover_name="packer"/>
		<Add mover_name="bckrub"/>
	</ParsedProtocol>
	<LoopOver name="loop" mover_name="pack_dock" iterations="10"/>
</MOVERS>
<APPLY_TO_POSE>
</APPLY_TO_POSE>
<PROTOCOLS>
	<Add mover="add_csts" />
	<Add mover_name="loop"/>
	<Add mover="rm_csts" />
	<Add filter_name="sasa"/>
	<Add filter_name="ddg"/>
</PROTOCOLS>
</ROSETTASCRIPTS>


Script used to model VI120 and VI130 inhibitors with restriction of
backbone movement of DHPH domain
<ROSETTASCRIPTS>
<SCOREFXNS>
</SCOREFXNS>
<TASKOPERATIONS>
	<InitializeFromCommandline name="ifcm"/>
	<ReadResfile name = "rrf"
filename="/nas02/home/l/y/lyayuga/Zdrklibrary/VAV_Zdrk/resfile/VAV_Zdrk_VI
20n30_DHPH.resfile"/>
	<RestrictToRepacking name="r2p"/>
</TASKOPERATIONS>
<FILTERS>
	<Sasa name="sasa" confidence="0"/> change confidence to 1 if you
want low-sasa structures ot be supressed
	<Ddg name="ddg" confidence="1" threshold="0"/>
	<ShapeComplementarity name="sc" confidence="0"/>
	<BuriedUnsatHbonds name="unsatH" confidence="0"/>
</FILTERS>
<RESIDUE_SELECTORS>
    <Index name="tyr49" resnums="49C" />
    <Index name="arg332" resnums="332B" />
</RESIDUE_SELECTORS>
<MOVERS>
	<FastRelax name="flax" repeats="5" task_operations="r2p,rrf"
batch="false" ramp_down_constraints="false" cartesian="false"
bondangle="false" bondlength="false" min_type="dfpmin_armijo_nonmonotone">
		<MoveMap>
			<Chain number="2" chi="1" bb="0"/> restrict backbone
movement for DHPH
		</MoveMap>
```

```
        </FastRelax>
        <DockingProtocol name="dock2" low_res_protocol_only="0"
docking_local_refine="0" dock_min="1" ignore_default_docking_task="0"
task_operations="r2p,rrf" partners="B_C"/>
        <AddConstraints name="add_csts" >
                <HydrogenBondConstraintGenerator name="gen_my_csts"
                residue_selector1="tyr49"
                residue_selector2="arg332"
                atoms1="OH"
                atoms2="NH1"
                atom_pair_func="FLAT_HARMONIC 2.6 0.1 0.5" />
         </AddConstraints>
         <RemoveConstraints name="rm_csts"
constraint_generators="gen_my_csts" />
        <Backrub name="bckrub"/>
        <PackRotamersMover name="packer" task_operations="ifcm,rrf"/>
        <Docking name="dock1" fullatom="1" local_refine="1"/> make
fullatom=0 to do low-resolution only docking. Change local_refine=1 to do
only high-resoltuion docking
        <ParsedProtocol name="pack_dock" >
               <Add mover_name="dock2"/>
               <Add mover_name="packer"/>
               <Add mover_name="bckrub"/>
               <Add mover="flax" />
        </ParsedProtocol>
        <LoopOver name="loop" mover_name="pack_dock" iterations="5"/>
        <SwitchResidueTypeSetMover name="fa_switch" set="fa_standard"/>
</MOVERS>
<APPLY_TO_POSE>
</APPLY_TO_POSE>
<PROTOCOLS>
        <Add mover="add_csts" />
        <Add mover_name="loop"/>
        <Add mover="rm_csts" />
        <Add filter_name="sasa"/>
        <Add filter_name="sc"/>
        <Add filter_name="unsatH"/>
        <Add filter_name="ddg"/>
</PROTOCOLS>
</ROSETTASCRIPTS>
```

Sample Purification Protocol

Batch Protein purification

1. Resuspend in 15mL GST wash buffer (w/ 1mM DTT)+ 2.5uL Lysozyme + protein inhibitor pallet

2. Sonicate 15s on/15s off for 3 mins on ice. (Reserve 20uL as Lysate fraction)

3. Transfer to 30 mL centrifuge tube

4. Spin 16,000 RPM 4C 35 minutes (Reserve 20uL supernatant as Cleared Lysate fraction)

Equilibrate resin

5. Add 1 mL of GST-agarose slurry to 15 mL falcon tube

6. Centrifuge for 2 min at 700 x g

7. Decant supernatant

8. Resuspend resin in 3 mL wash buffer

9. Centrifuge for 2 min at 700 x g

10. Decant supernatant

11. Resuspend reins in 3 mL wash buffer

12. Centrifuge for 2 min at 700 x g

13. Decant supernatant (Do this immediately before the following step so that the resin does not out)

Incubation

13. Add clarified lysate to washed resin

14. resuspend resin.

15. rotate end over end for 1 h (reserve 20 uL)

Column

16. Add entire sample to column (collect 20 uL of flow through)

17. Wash with 5 mL of wash buffer (collect 20 uL of wash)

18. Add 1 mL Elution buffer to top of column

19. Allow to drain into 1.5 mL microfuge tube (Elution fraction 1)

20. Add 1 mL Elution buffer to top of column

21. Allow to drain into 1.5 mL microfuge tube (Elution fraction 2)

22. Add 1 mL Elution buffer to top of column

23. Allow to drain into 1.5 mL microfuge tube (Elution fraction 3)

References

[1] Jo¨ Rg, Birkenfeld. et al. (2008) Trends in Cell Biology 18.5: 210-219. [2] Rossman K et al. (2005) Nat Rev MCB. 6:167–180. [3] Ridley, Anne J. (2011) Cell 145.1: 1012-1022. [4] Raftopoulou et al. (2004) Developmental Biology 265.1: 23-32. [5] Cullis, Jane. et al. (2014) Cancer Cell 25.1: 181-195. [6] Cardama, G.a., et al. (2018) Critical Reviews in Oncology/Hematology. 124: 29–36. [7] Sebban S et al. (2013) PLoS One. 8:54321. [8] Leaver-Fay A et al. (2011) Meth. Enzymol. 487:545–574. [9] Wang H et al. (2016) Nature Methods. 13: 755-758. [10] Davis IW et al. (2006) Structure. 14:265-274 [11] Chao, Ginger et al. (2006) Nature Protocols. 1: 755-68. [12] Crespo, Piero, et al. (1997) Nature. 385: 169–172. [13] Hallett RA et al. (2016) ACS Synth Biol 5:53–64. [14] Katzav S (2015) Oncotarget. 6: 28731–28742. [15] Mihai LA (2011) Science. 334:373-376. [16] Fleishman SJ et al. (2011) Science. 332: 816–821. [17] Jacobs TM et al. (2016) Science. 352:687–690. [18] Jacobs TM et al. (2015) Nucleic Acids Research 43:e34–e34. [19] Rocklin, GJ et al. (2017) Science, 357: 168-175. [20] Evelyn CR et al. (2014) Chem Biol. 21: 1618–1628. [21] Heck, Jessica N. et al. (2012) Molecular Biology of the Cell 23.1: 2583- 2592.